Further evidence for a relatively high sea level during the penultimate interglacial: open-system U-series ages from La Marina (Alicante, East Spain)

José L. Goy [a]; Claude Hillaire-Marcel [b]; Cari Zazo [c] *; Bassam Ghaleb [b]; Cristino J. Dabrio [d]; Ángel González [a]; Teresa Bardají [c]; Jorge Civis [a]; Michel Preda [b]; Alfonso Yébenes [f]; Alessandro M. Forte [b]

Abstract

The elevation and timing of high sea stands during Oxygen Isotope Stage (OIS) 7 are not as well constrained as those of OIS 5e. Conflicting values are reported from Mediterranean coastlines, and fossil dating is inaccurate because of ubiquitous open U-series systems. New morphostratigraphic data from La Marina (eastern Spain) supported by open-system U-series coral ages shed light on the maximum sea level during OIS 7. Fossil corals (*Cladocora caespitosa*) underlying an OIS 5e marine unit yielded U-series ages from 178 ± 10 to 208 ± 11 ka (±2σ; n=7) with an outlier at 240 ± 18 ka. Mean open-system limit ages of 170 ± 10 (minimum age after correction for ^{234}Th - ^{230}Th uptake) and 237 ± 20 ka (maximum age after correction for ^{238}U - ^{234}U uptake) were calculated to have a probable age closer to the minimum value, for an assignment of OIS 7a or 7c. The occurrence of a warm-water "Senegalese" fauna (*Strombus bubonius*) in OIS5e and OIS 7 marine units confirms the arrival of tropical species to the Mediterranean before the last interglacial period. Morpho-sedimentological and neotectonic studies suggest that the maximum paleo-sea level during OIS 7c or 7a was a few meters below that of OIS 5e.

Keywords: Oxygen isotopic stage 7, Western Mediterranean, *Cladocora caespitosa*, "Senegalese" fauna, neotectonics

1. Introduction

Long-term climate modelling requires an in-depth understanding of the interactions among climate dynamics, greenhouse gases, sea level, ocean changes and ice volume. Thus, independent information on the evolution of each of these Earth system components at different time scales is very useful. From this viewpoint, the elevation and timing of high sea stands in the last interglacial (OIS 5e); (e.g. [1-6]) are better documented as those of the penultimate interglacial (Oxygen Isotope Stage: OIS 7) [7-19]. Largely discordant values have been reported for the maximum absolute elevation during each of the OIS 7 high sea stands and, due to the opening of the U-series systems in fossil indicators, their precise dating remains a problem. The development of open-system U-series age models [20] now allows us to determine more accurately ages in the OIS 7 time range.

Using proxy data such as the stacked benthic foraminiferal $\delta^{18}O$ curve of SPECMAP [21, 22], one cannot precisely determine the maximum elevation of the OIS 7 sea level relative (near or much below) to that of OIS 5e, notably with reference to substage 7c $\delta^{18}O$-values, because it is difficult to decouple the ice volume and the temperature signals in the oxygen isotope record. The best preserved remnants of OIS 7 sea stands are not necessarily coeval with the short substages during which paleo-sea levels reached a maximum elevation (Substages 7c or 7a); instead, they could correspond to episodes when sea levels were well below OIS 5e datum, for example during Substages 7b and 7e.

Sequences of staircased terraces from tectonically active areas, such as New Guinea [23] or Barbados [11], could help to decipher the number and relative elevations of all stillstands during the relatively high sea levels of OIS 7, but the many uncertainties in the rate and mode of uplift largely impedes to assess the relative elevations of the corresponding absolute paleo-sea levels.

This contribution presents new morphostratigraphic data from raised marine units at La Marina-El Pinet (at the Spanish coast of the Western Mediterranean Sea, Fig. 1 A, B and C) accompanied with high precision U-series measurements in fossil corals (*Cladocora caespitosa*) found in the same layer as *Strombus bubonius*. These data provide critical information on the elevation of (at least) a *maximum* sea level of OIS 7, relative to that of OIS 5e, and sea surface temperatures (SST) in the western Mediterranean during OIS 7 and OIS 5.

In this study, we also intend to discuss further U-correction models in situations where diagenetic U-uptake may have occurred in parallel with ^{234}Th - ^{230}Th enrichments, as documented in recent times [20 and 24].

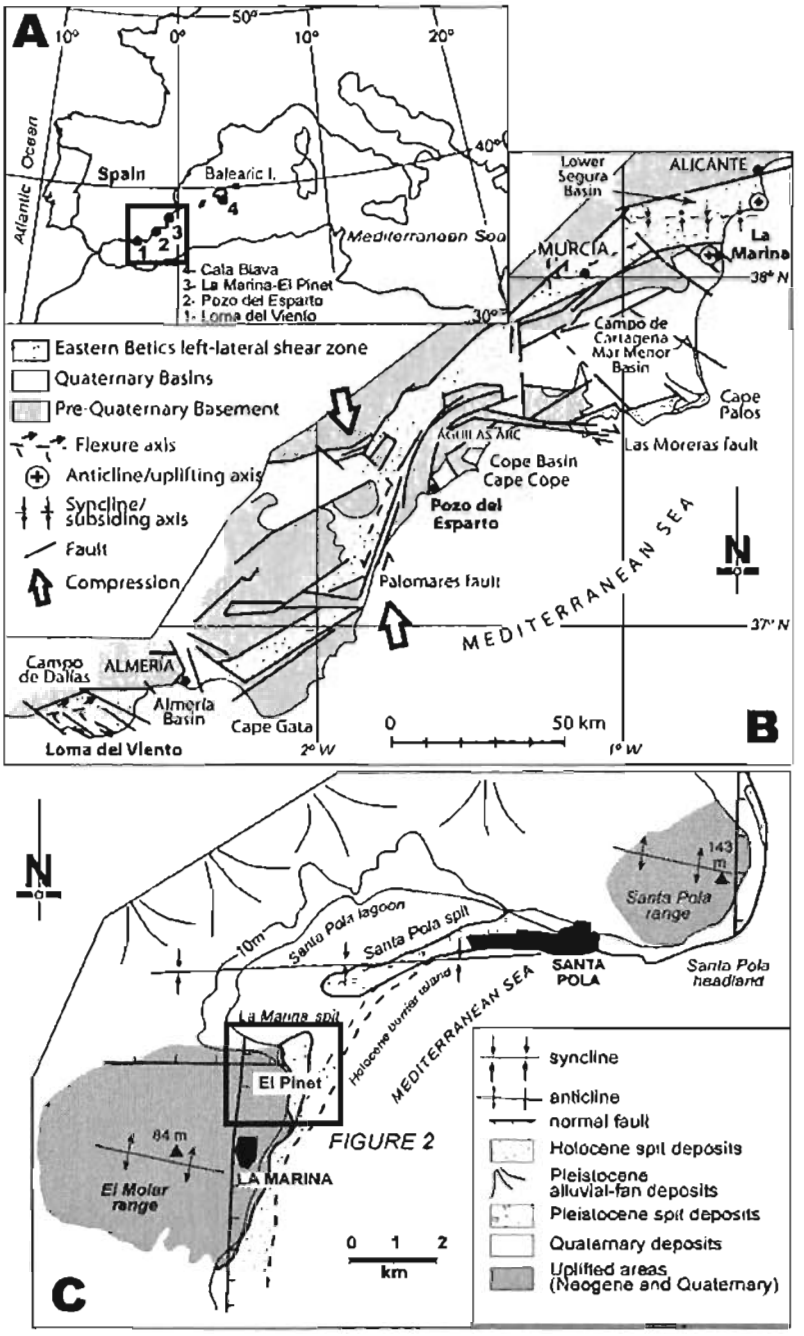

Figure 1.- (A) Location map of the study area (La Marina-El Pinet, see B) and other sites with OIS 7 deposits cited in this paper; (B) Location of the studied zone in the eastern Betic Cordillera; (C) Location of La Marina-El Pinet area with the main E-W structures affecting Quaternary terrestrial and marine deposits.

2. The Upper Quaternary littoral deposits at the La Marina-El Pinet site

2.1. Geological and geomorphological settings

La Marina-El Pinet area is located in the northern termination of the so-called Eastern Betics Shear zone (Fig. 1B), where transpressional basins show a deformation of their oldest

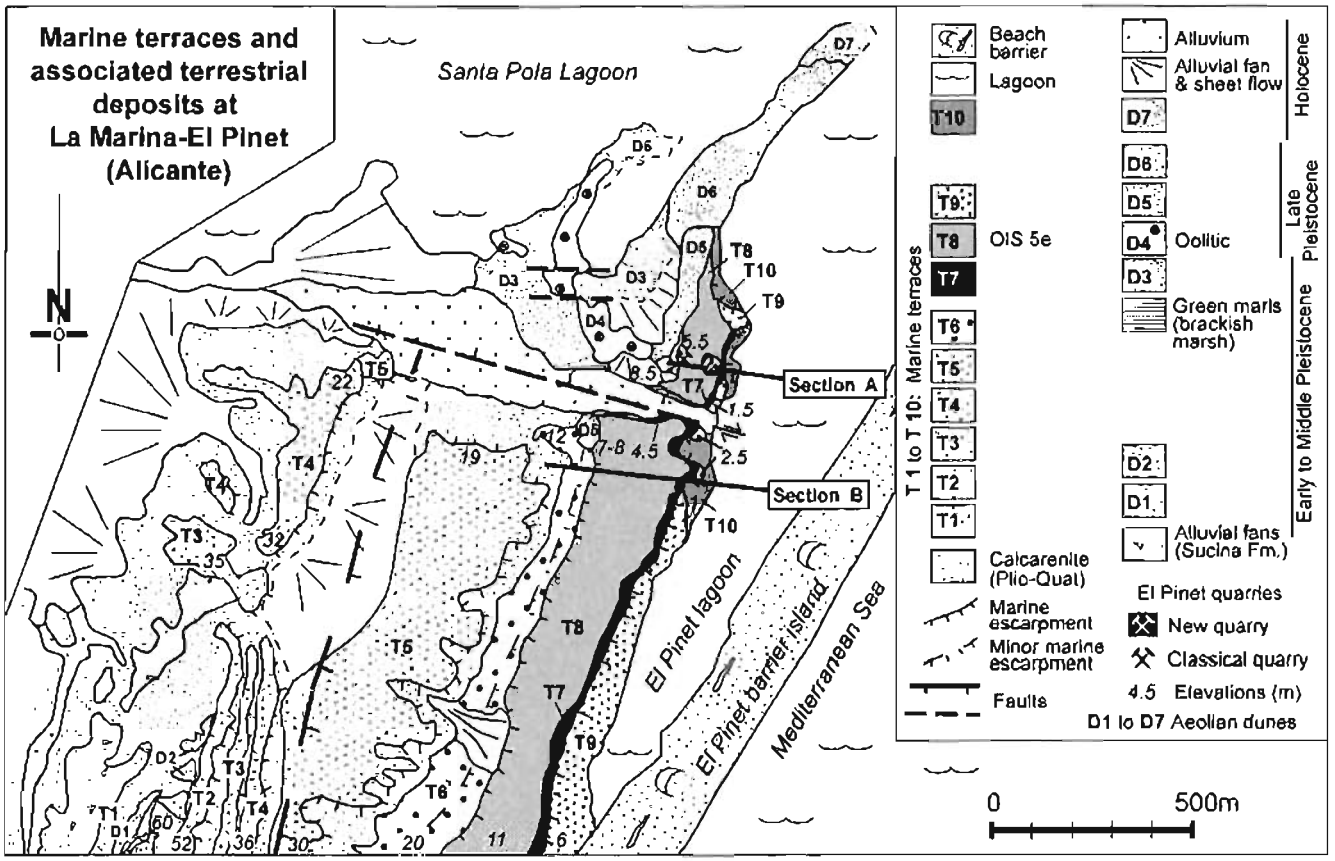

Figure 2.- Geomorphologic map of La Marina –El Pinet with indication of sections presented in Fig. 3

Quaternary deposits in wide E-W trending folds and flexures [25]. An early-middle Pleistocene neotectonic event triggered the uplift of the anticlinal folds promoting the encasement of flights of marine terraces in the sea-facing slopes of the growing hills at La Marina, while N-S faults controlled the coastal outline [25, 26]. In this geodynamic framework, at least ten Quaternary marine terraces (informally named T1 to T10) were recognized in La Marina (Fig. 2), with elevations progressively decreasing towards the East from 60 m above sea level (T1) to 0 m (T10). The scarps separating successive marine terraces decreased with time, being larger in the oldest terraces than in the younger ones. A normal fault directed WNW-ESE, with the downthrown block to the north, divides the staircase. The quarries presented are placed in the downthrown fault block (Fig. 2). This paper deals with terraces T7 and T8.

2.2. *Earlier studies*

One of the most repeatedly studied sites in the Alicante-Almeria area (western Mediterranean basin, Fig. 1) is a shallow excavation, commonly referred to as "El Pinet Quarry" (called in this paper the "classical" El Pinet Quarry (Fig. 2), located 2 km north of La Marina resort (Fig 1C). Most coastal sediments in the quarry contain a faunal association including the gastropod *Strombus bubonius*, commonly referred to as "Senegalese" fauna, indicative of warm-water conditions [e.g. 27].

Early U-series measurements on *S. bubonius* shells at El Pinet Quarry by Bernat *et al.* [28] yielded ages ranging from 150 to 65 ka, with a cluster of values around 98 ± 5.8 ka (± 1σ) that led these authors to propose an OIS 5c age for all marine deposits of the quarry. Hearty *et al.* [29] sampled the quarry for Amino-Acid Racemization (AAR) analyses and distinguished two marine units bearing the "Senegalese" fauna with *S. bubonius*. Fossils from Unit I, at +3 m above sea level (a.s.l.), were assigned to aminozone E, considered to represent OIS 5e (ca 125 ka). Fossils from Unit II, at +2.5 m a.s.l., were assigned to aminozones F and G, with ages likely to be from stages 7 and 9 or older, as deduced from other Mediterranean sites.

Multidisciplinary studies by Goy and Zazo [25, 26] and Goy *et al.* [30] refined the stratigraphic and tectonic frameworks and recognized at least three highstands within OIS 5 deposits, representing presumably OIS 5e (oolitic), 5c and 5a (biocalcarenitic). Conditions favourable to the formation of oolitic facies (warm, shallow waters with more or less horizontal sea floor) were found along the Spanish Mediterranean coast exclusively during the Late Miocene [31] and during OIS 5e [30]. U-series measurements [32] in samples collected from the oolitic and the calcarenitic units revealed a great variation in the concentrations of U, similar to those found by Bernat *et al.* [28].

More recently, Zazo *et al.* [19] reported on shallow marine sediments hosting colonies of the coral *Cladocora caespitosa*

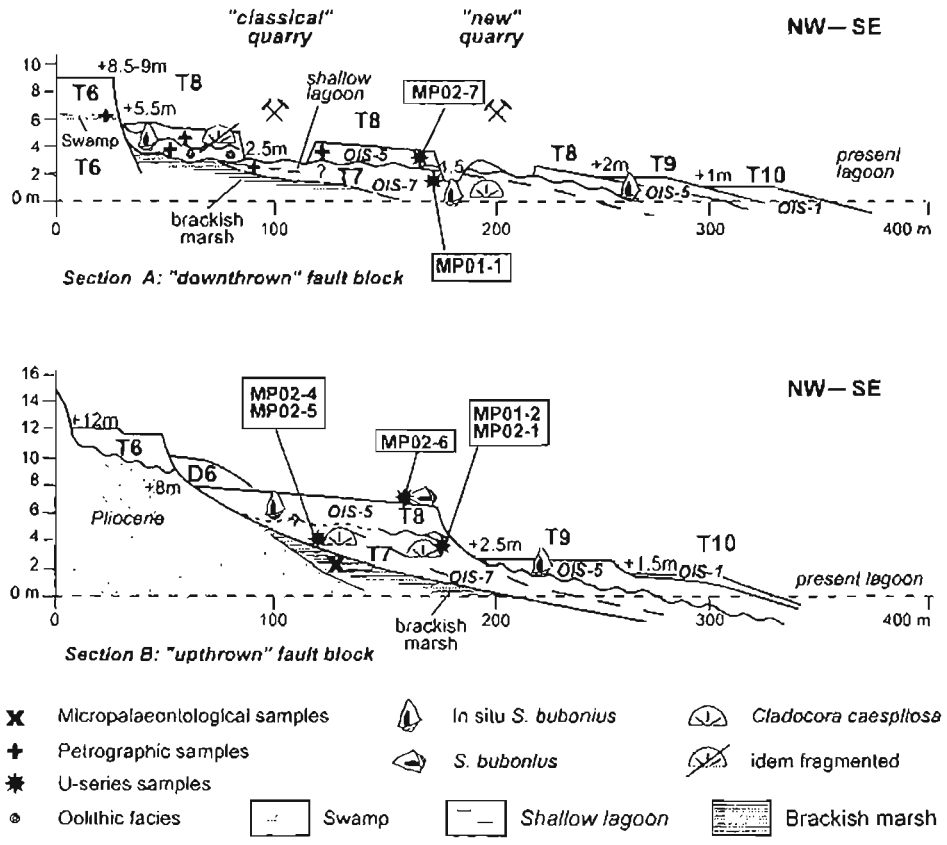

Figure 3.- Cross sections that illustrate the differences in the sedimentary record at both sides of the E-W fault (A: downthrown, B: upthrown fault blocks). Distances measured with metric tape, elevations with theodolite and rod. The datum is the high-water mark of the tideless El Pinet lagoon. Note that the exaggerated vertical scale necessary for improving visualization confers the drawing a somewhat sketchy, cartoon-like appearance.

accompanied with scarce *S. bubonius* at a "new" El Pinet Quarry (Fig. 2), some 100 m ESE from the "classical" El Pinet Quarry. The interesting fact is that they occur stratigraphically below the deposits exposed in the "classical" site. Preliminary U-Th measurements yielded an age of 178 ± 10 ka (±2 σ) for the *Cladocora* colonies, thus suggesting their growth occurred during OIS 7. These authors re-evaluated the regional context, the sedimentary facies, and the published numerical (U-series) and relative (AAR) ages, and proposed an OIS 5e age for all the oolithic and biocalcarenite deposits exposed at La Marina-El Pinet "classical" Quarry.

2.3. Methods and material

The present study is supported by geomorphologic, sedimentological, palaeontological, and neotectonic analyses coupled to new U-series measurements on fossil *C. caespitosa* colonies and *S. bubonius* shells. In order to reconstruct the local palaeogeography during deposition of the marine terrace (T7) that hosts both *C. caespitosa* and *S. bubonius*, a new detailed mapping of the area including geological, morphological and neotectonic features of the Quaternary deposits was conducted (Fig. 2). Mapping was based on aerial photographs scaled at 1:18,000 and 1:5,000, with field checking. The datum for topographic elevations is the high-water mark of the almost tideless Mediterranean sea (astronomical tidal ranges do not exceed 10 cm in Alicante). The topographic elevation of marine terraces above sea level refers to the altitude of the inner (most inland) part of the marine wedge, or "shoreline angle". It is indicated on the map (Fig. 2) with numbers in italics, and in the sections (Fig. 3) with numbers preceded by a "+" symbol. Facies analysis of the foreshore-shoreface transition, particularly the plunge-step zone, offers a reliable indicator of the relative sea level at the time of deposition. It was supplemented by palaeontological studies and petrographic observations of thin sections aimed at reconstructing the coastal environments when the marine terraces formed.

2.4. Marine terraces at El Pinet area

The mapped marine terraces crop out as adjacent strips trending NNE-SSW, i.e., parallel to the present coastline (Fig. 2). From T6 onwards, the marine terrace deposits in the southern block of the WNW-ESE fault are generally thinner and neatly separated, whereas those in the northern downthrown block are thicker and vertically stacked or amalgamated, indicating that sediment deposition coincided with the time of fault movement.

Terraces T1 to T6 consist of well-cemented conglomerates, some of them rich in *Ostrea*, *Balanus*, and *Glycymeris* [19]. In contrast, the fossiliferous sands and conglomerates of terraces T7 to T10 are poorly cemented.

Terrace T6 (cemented coastal-to-marine conglomerates rich in *Glycymeris sp.*) exceeds 7 m in thickness on the northern, downthrown fault block, where is divided into two distinct subunits by a 50 cm-thick intervening layer of grey-yellowish sandy marlstones (Fig. 3, Section A). Petrographic criteria (pedogenic crusts with calcrete-like layers, microsparitic cements, pedotubules, and ferruginous staining of micrite cements) point to deposition in a swamp environment. In contrast, T6 deposits on the southern, uplifted, fault block consists of 3 m of conglomerates, divided into two smaller terraces by a low escarpment (Figs. 2 and 3, Section B).

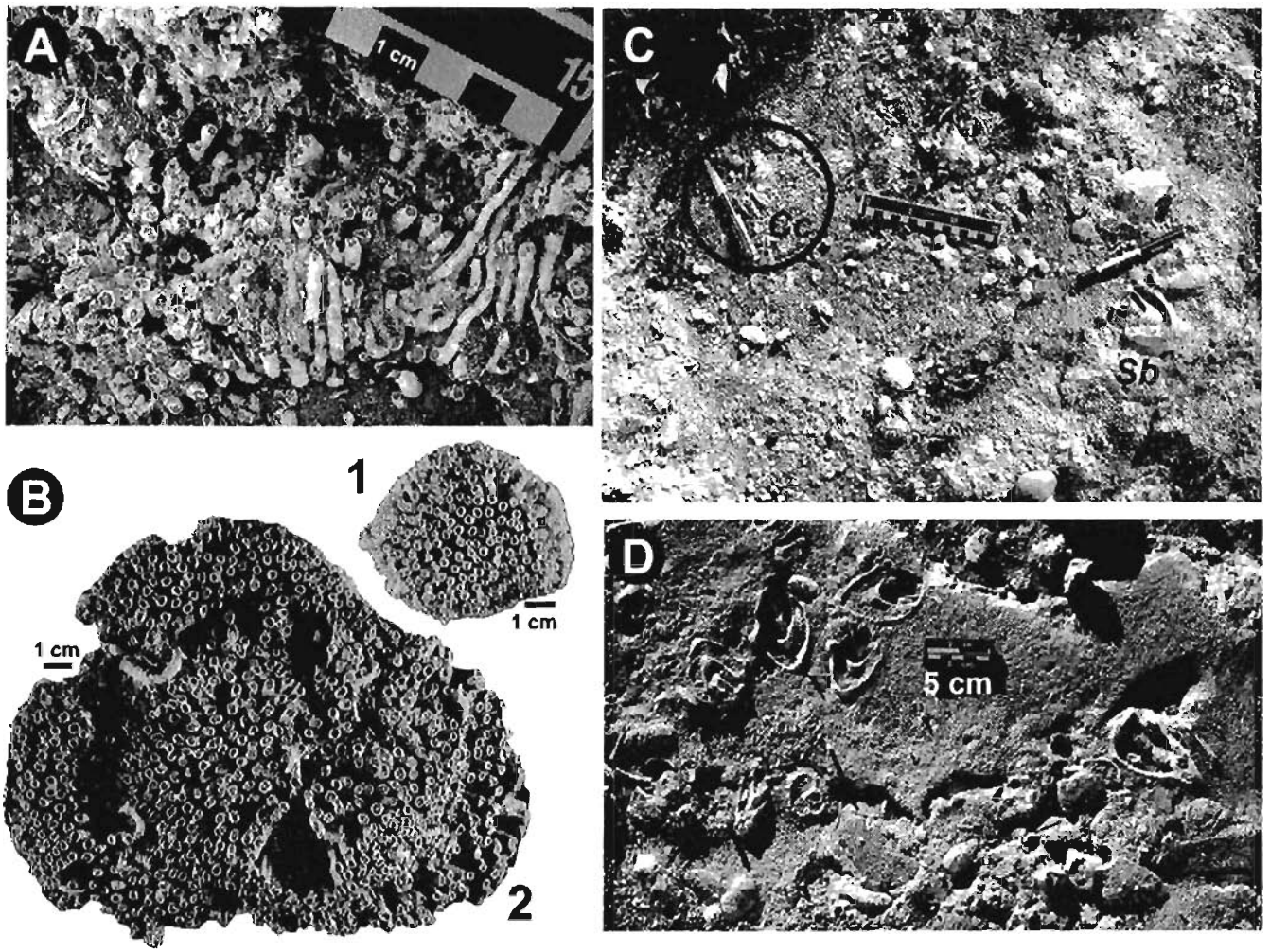

Figure 4.
(A) Fossil *C. caespitosa* of OIS 7 age (shoreface facies of terrace T7 at La Marina-El Pinet) from which samples labelled MP01-2 and MP02-1 were taken for U-series measurements.
(B1) Present *Cladocora caespitosa* living at 3m water depth (Cala Blava, Mallorca Island) where U-series sample MCB02 was collected.
(B2) Present *Cladocora caespitosa* living at 6m water-depth (La Manga del Mar Menor, Murcia) where U-series sample MMM02 was collected (both specimens from the collection of the Museo Nacional de Ciencias Naturales, Madrid, CSIC).
(C) Shoreface deposits (OIS 7) hosting *Cladocora caespitosa* and *Strombus bubonius* from the "new" El Pinet Quarry (T 7, see Fig. 3 section A).
(D) *Strombus bubonius* in oolitic deposits dated as OIS 5e at the "classical" El Pinet Quarry (T 8, see Fig. 3 section A).

The whole set of terraces T7 to T10 is bounded by an erosional escarpment (a paleo-cliff) that forms the seaward limit of the well-cemented terrace T6. Erosion and encasement took place before sedimentation of T7, and greenish sandy silts occur encased in T6, but underlying the onlapping T7 (Fig. 3). A rich oligohaline ostracofauna (*Hyocypris bradyi*, *Candona sp.*, *Cyprideis torosa*, *Limnocythere inopinata*, *Paralimnocythere rostrata*), benthic foraminifera, and scarce oogons of charophytes, suggests deposition in a brackish marsh, with limited marine influence witnesses by small-sized planktonic forams.

Terrace T7 is exposed at the surface in erosional "windows" of the overlying Terrace 8, reaching maximum heights of 1.5 m a.s.l. and 4.5 to 5 m a.s.l. in the downthrown and upthrown fault blocks, respectively. Deposits of T7 consist of fossiliferous calcarenites, silty sands, and some conglomerates. These sediments host the coral *Cladocora caespitosa* (Fig. 4A) both as small patches, one metre across and up to 30 cm in height, and as hemispherical colonies some 15 cm in diameter, similar to those living in the western Mediterranean (Fig. 4B 1 and 2). Molluscs (*Ostrea*, *Bittium*, *Rissoa*) are commonly associated with the coral colonies. There are also scarce specimens of the "Senegalese" fauna (*Cantharus viverratus*, *Conus testudinarius*, and *S. bubonius*, Fig. 4C). The contact separating T7 from T8 is an irregular, erosional, encrusted surface visible at the "new" El Pinet Quarry (Fig. 5A). A discontinuous layer of wackestone facies with fine quartz grains crops out at the lowermost part of the "classical" quarry below the oolitic facies (T8) but could not be traced laterally to the "new" quarry (Fig. 3, Section A). Faunal content (serpulid-worm tubes, remains of gastropods) and moulds very much alike plant-root replacement suggest deposition in a shallow lagoon that was likely located landward of the barrier beach deposits where the *Cladocora* colonies lived.

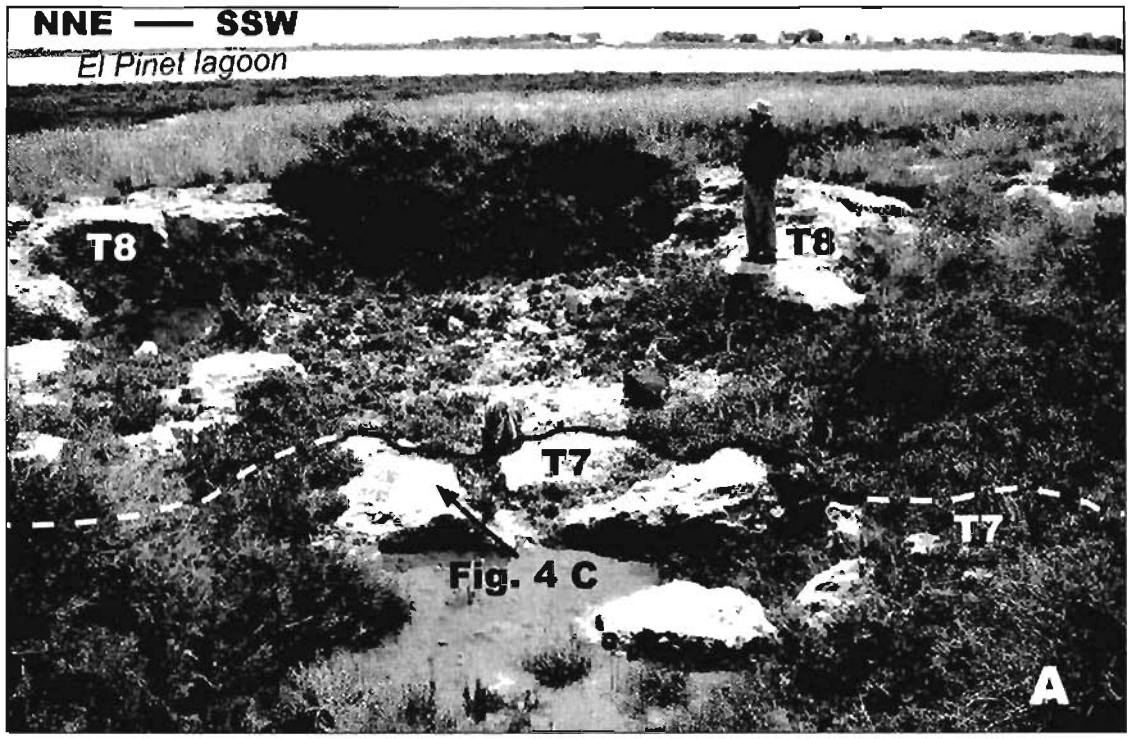

Figure 5.
(A) Panorama of the shallow excavation referred to as the "new" El Pinet Quarry and the boundary between marine terraces T7 and T8. The outcrop of biocalcarenites bearing *C. caespitosa* and *S. bubonius* (see Fig. 4C) is in the centre of the picture. The man is 1.75m tall.

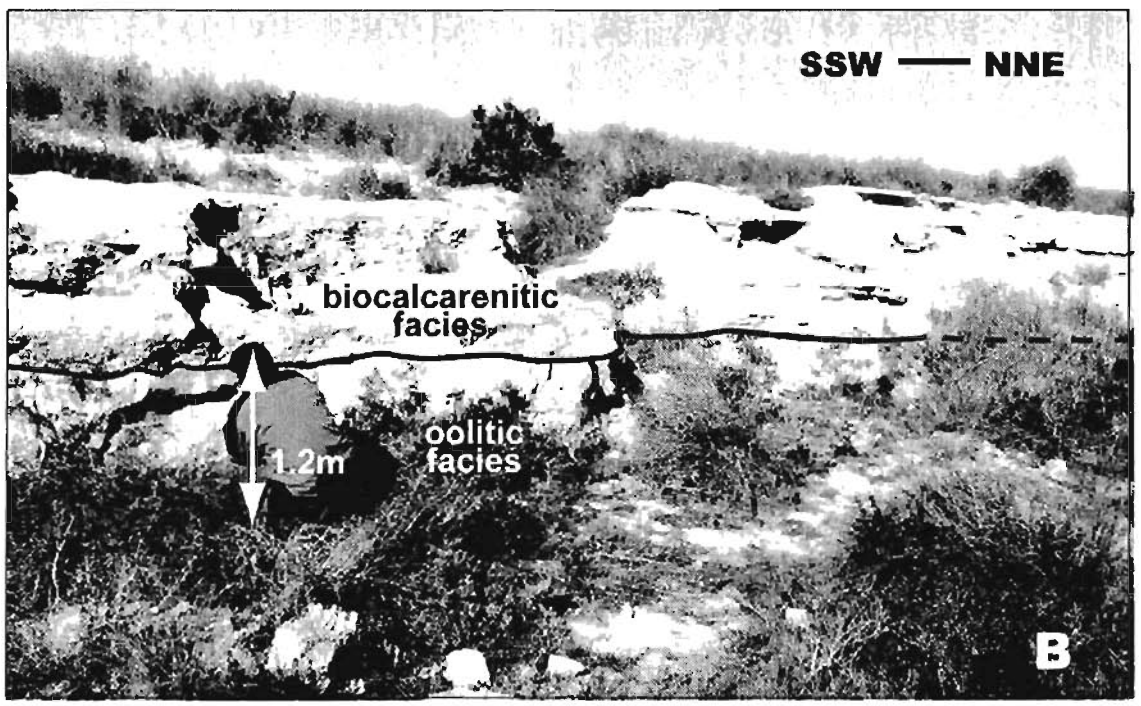

(B) The panorama of the "classical" quarry showing the boundary between the oolitic and biocalcarenitic facies (Terrace T8).

Terrace 8 is topographically higher than T7; its inner margin culminates at 5.5 m a.s.l. and 8 m a.s.l. in the downthrown and upthrown fault blocks, respectively. T8 includes two subunits separated by an erosional surface ("classical" quarry in Fig. 3, Section A, and Fig. 5B): a basal oolitic facies and an overlying bio-calcarenite facies, both rich in the "Senegalese" fauna, especially *S. bubonius* (Fig. 4D), repeatedly collected for U-series and AAR dating [28, 29, 30, 32 and 12].

Terrace T9 consists of calcarenite and conglomerates with an abundant "Senegalese" fauna. The inner margin is located at +2 m a.s.l. in the downthrown block and +2.5 m a.s.l. in the upthrown block (Fig. 3, Sections A and B).

The bioclastic terrace T10 bears a fauna identical to the modern one, and is located at +1 m a.s.l. and +1.5 m a.s.l. in the downthrown and upthrown blocks, respectively (Fig. 3, Sections A and B).

Table 1: U-series measurements in samples from La Marina-El Pinet

		Mineralogy (%)*				$[^{238}U]$	$[^{232}Th]$	$^{234}U/^{238}U$	$^{230}Th/^{234}U$	Age (ka)	$(\delta^{234}U)_0$
		Cal.	Mn-C	Arag.	Qtz	ppm	ppb				‰
La Marina north block (new quarry) – Lower marine sequence (T7)											
MP01-1a	*C. caespitosa*	87.6	1.38	1.61	2.30	2.598±0.011	92.9±1.2	1.115±0.004	0.837±0.013	185.2+7.8/-7.2	195±8
MP01-1b	*C. caespitosa*	13.2	10.0	56.5	1.61	2.755±0.013	130.1±1.0	1.129±0.010	0.843±0.013	187.8+8.4/-7.7	220±18
MP01-1c	*C. caespitosa*	----	----	----	----	2.458±0.011	138.3±1.3	1.120±0.006	0.857±0.008	196.6+5.6/-5.3	210±10
MP01-1d	*C. caespitosa*	----	----	----	----	2.915±0.023	142.9±1.8	1.099±0.011	0.822±0.016	178.2+9.8/-8.9	165±18
La Marina south block (new section) – Lower marine sequence (T7)											
MP01-2	*C. caespitosa*	56.0	0.84	26.4	3.64	2.737±0.021	246.0±2.5	1.132±0.009	0.918±0.017	239.8+18/-16	261±18
MP02-1	*C. caespitosa*	49.4	15.3	20.9	6.12	2.549±0.016	65.97±0.61	1.109±0.012	0.871±0.014	207.6+11/-10	194±21
MP02-4	*C. caespitosa*	19.6	1.29	64.0	7.18	3.234±0.017	201.5±2.2	1.118±0.007	0.852±0.011	194.5+7.8/-7.2	202±12
MP02-5	*C. caespitosa*	25.9	50.8	6.47	11.0	2.639±0.014	92.5±1.0	1.119±0.011	0.843±0.013	189.5+8.8/-8.1	201±18
Mean value for *C. caespitosa* (±1σ)						2.736±0.229					
La Marina – Upper marine sequence (T8)											
MP02-7	*S. bubonius*	-----	----	-----	----	0.7280±.0045	4706±46	1.352±0.012	0.596±0.007	93.7±1.8	459±119
MP02-6	*S. bubonius*	----	-----	----	-----	0.3157±.0022	3760±50	1.330±0.012	0.694±0.013	120.1±4.2	464±146

Note: all values are quoted at ±2σ level of uncertainty

* Total ≤ 100% due to the presence of traces of other contaminating minerals. Cal: calcite; Mn-C: Mn-calcite; Arag.: aragonite; Qtz: quartz.

3. U-Series measurements

3.1. Samples and laboratory procedures

U-series measurements were performed on several specimens of *C. caespitosa* from terrace T7 deposits at La Marina-El Pinet, as well as on some modern specimens from the Mediterranean, that were provided by the *Museo Nacional de Ciencias Naturales* of Madrid. Samples MP01-1 a through d were taken from different parts of the same colony (Section A; Fig. 3). Samples MP01-2, MP02-1, 4 and 5 were collected in another section (Fig. 3, Section B) from two distinct patches some 50 meters apart from each other. Measurements were also performed on a couple of specimens of *Strombus bubonius* (MP02-6 and 7) collected from the marine terrace T8, that directly overlies the *C. caespitosa* bearing unit (Fig. 3, Sections A and B). *C. caespitosa* seems absent in this upper unit, except for a few fragments possibly reworked from the lower unit.

Calcite and other mineral percentages in coral carbonates were determined by X-ray diffraction (XRD) using a Siemens D5000 with Co Kα1,2 radiation and a Si detector. Samples (~ 10–50 mg) were grounded to fine particles (~5 μm in diameter) through hand grinding. A mount was then prepared by smearing the particles with distilled water on to a silicon plate, and then air-dried. The goniometer scans from 5° to 50°2θ with a step size of 0.01°2θ and a count time of 2 s/step for all samples. Following a first screening run, NIST 640C-Si powder was added to the sample for proper calibration of the second run used for final measurements. Tube voltage and current were respectively set at 40 kV and 30 mA. Diffractograms were stripped to remove Kα2 signal. Mineral weight percentages were calculated by the integrated peak intensity procedures following Cook *et al.* [33]. Magnesium content in skeletal carbonate was determined from the displacement of the *d*104 peak of calcite with increasing $MgCO_3$ [34]. Potential changes in the Co Kα1,2 radiation were regularly checked using a Si-Standard mount. Precision of XRD through the whole experiment was estimated by measuring the positions of the *d*111 and *d*220 peaks of silicon before and after a sequence of daily analyses (5 samples) and was better than ±0.01°2θ. This implies that concentrations determined by XRD are accurate to ±2 mol% calcite.

Analytical procedures for U and Th separation followed Edwards *et al.* [35], with a modified two stage extraction with 6 N HCl and 7N HNO_3 to increase the yield of U (see [36] for more details). Measurements were made on a VG-Sector thermal ionization mass spectrometer equipped with an electrostatic filter and an ion-counting device. The overall analytical reproducibility as estimated from replicate measurement of standards is usually better than ±0.5% (±2σ error) for U and Th concentrations as well as for $^{234}U/^{238}U$ and $^{230}Th/^{234}U$ ratios (Tables 1 and 2).

3.2. Results

Analytical results are summarized in Tables 1 and 2. All *C. caespitosa* samples yielded U concentrations in a range expected for Scleractinian, aragonitic corals (mean [U] = 2.736±0.229 ppm), but with an excess of ^{234}U *vs.* ^{238}U (mean $\delta^{234}U_0 = 206\pm27$) exceeding values expected for purely "marine" uranium at the origin (*cf.* $\delta^{234}U = 148 \pm 4$ in modern specimens; Table 2). One peculiar feature of the coral fragment analyzed is their highly variable content in calcite (*vs.* aragonite) as well as in subsidiary minerals, notably quartz ranging 1.6 to 11 %, indicating that cleaning procedures were not efficient enough to remove all detrital

Table 2: U-series measurements in Last Interglacial [44 and 45] and modern *Cladocora caespitosa* samples.

	[^{238}U] ppm	^{234}U/^{238}U	^{230}Th/^{234}U	Age (ka)	$(\delta^{234}U)_0$ ‰	Source
Modern samples (values from TIMS measurements quoted at ±2σ level of uncertainty)						
MMM02 (SE Spain)	2.560±0.022	1.142±0.010			142±10	Present study
MCP02-1 (Mallorca)	3.278±0.029	1.148±0.009			148±9	Present study
MCB02 (Mallorca)	3.041±0.027	1.154±0.009			154±9	Present study
IC02 (Eastern Spain)	3.102±0.027	1.148±0.008			148±8	Present study
Mean values (±1σ)	2.995±0.266	1.148±0.004			148±4	
Last interglacial samples (values obtained from α-counting measurements quoted at ±1 σ level of uncertainty)						
Las Huertas (SE Spain)	3.62±0.07	1.106±0.014	0.744±0.021	142.9+9.1/-8.3	159±67	Szabo in [45]
Son Grauet (Mallorca)	3.00±0.05	1.112±0.014	0.702±0.021	127.6+7.8/-7.2	161±63	Szabo in [45]
Calamosca (Sardinia)	3.67±0.07	1.112±0.018	0.735±0.017	139.3+7.3/-6.8	166±72	Szabo in [45]
Monastir (Tunisia)	3.48±0.07	1.104±0.017	0.697±0.021	126.2+7.8/-7.2	149±62	Szabo in [45]
Mare Piccolo (SE Italia)	3.76±0.06	1.114±0.017	0.682±0.020	121.0+7.1/-6.6	161±64	Szabo in [45]
Mean values (±1σ)	3.51±0.27	1.110±0.004			159±6	
Paphos (Cyprus)	2.49	1.09±0.02	0.66±0.01	114.8+3.6/-3.4	125±54	[44]
Paphos (Cyprus)	2.36	1.09±0.03	0.66±0.02	114.8+7.1/-6,5	125±63	[44]
Paphos (Cyprus)	2.06	1.17±0.03	0.64±0.02	107.3+6.3/-5.8	230±88	[44]
Paphos (Cyprus)	2.65	1.08±0.02	0.67±0.01	118.1+3.8/-3.6	112±51	[44]
Paphos (Cyprus)	2.65	1.09±0.02	0.70±0.01	127.6+3.8-3.6	129±48	[44]
Dhekelia (Cyprus)	2.10	1.10±0.01	0.73±0.01	137.9+4.2/-4.0	148±57	[44]
Dhekelia (Cyprus)	2.30	1.09±0.01	0.69±0.02	124.3+7.1/-6.7	128±46	[44]
Dhekelia (Cyprus)	2.13	1.10±0.02	0.73±0.01	137.9+4.6/-4.3	148±67	[44]
Dhekelia (Cyprus)	2.35	1.12±0.04	0.69±0.01	132.6+8.3/-7.5	170±89	[44]
Dhekelia (Cyprus)	2.01	1.15±0.03	0.72±0.02	121.0+7.1/-6.6	218±96	[44]
Mean values (±1σ)	2.31±0.23	1.11±0.03	0.69±0.03		153±41	[44]

Key: **MMM:** Mar Menor (Murcia); **MCP:** Cabo del Pinar (Mallorca); **MCB:** Cala Blava (Mallorca); **IC:** Islas Columbretes (Castellón).

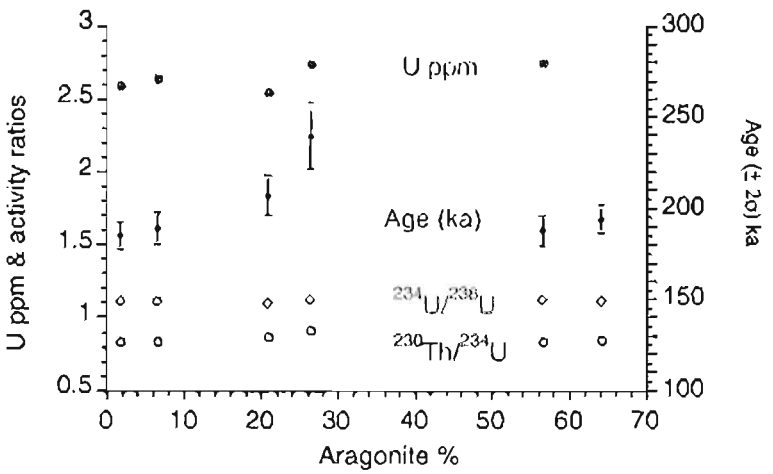

Figure 6.- Aragonite percentage in coral skeletons (data from Table 1) *vs.* ^{230}Th-ages, U concentrations and activity ratios (see text).

particles from fossil skeletons. Despite the presence of large amounts of replacement calcite (Table 1), U concentrations and activity ratios are totally independent of calcite contents in samples (Fig. 6), suggesting that the mineralogical transformation occurred without significant uptake/loss of uranium, thus with minimum impact on U-series systematics. The relative abundance of a Mn-bearing calcite indicated by X-Ray analysis (Table 1) would indicate some bacterial influence in the process of aragonite replacement. In a recent paper, Pons-Branchu *et al.* [37] have illustrated similar early diagenetic changes in deep corals due to bioerosion and secondary biomineralization processes. Nevertheless, minimum U-mobility may have occurred in these samples, likely during a very early diagenetic stage. They will be discussed below.

A common feature of the deposits of terraces T7 to T10 is a weaker cementation than that of the older terraces. This may have resulted in U-mobility and thus account for the scatter of ^{230}Th-ages and U contents in *S. bubonius* shells from OIS 5e deposits of the El Pinet "classical" quarry yielded by early measurements from Bernat *et al.* [28]. New measurements in two samples from terrace T8 also depict similar features, in particular in the most altered and porous of these fossil samples (MP02-7 in Fig. 7). The *S. bubonius* shells from this area provide an almost ideal illustration of an "open system" as illustrated in Figure 8, where decreasing

Table 3: U-series (α-counting) measurements in mollusk shells from cemented marine deposits of sites showing *Strombus bubonius*-bearing units assigned to the isotopic stage 7

	Elevation (m)	[^{238}U] ppm	^{234}U/^{238}U	^{230}Th/^{234}U	^{230}Th/^{232}Th	Age (ka)
Pozo del Esparto (from [32]) – IS 7 unit						
S. bubonius	7	0.35±0.01	1.24±0.03	0.95±0.03	155±24	252+28/-28
S. bubonius	7	1.10±0.03	1.24±0.04	0.88±0.04	309±11	200+31/-24
S. bubonius	7	0.56±0.01	1.18±0.04	0.87±0.03	57.4±0.9	199+25/-20
Cala Panizo (from [32]) – IS 5 unit						
S. bubonius	3	1.30±0.02	1.11±0.02	0.62±0.02	43±6	103±6
(All values are quoted with 1 standard deviation)						
Punta Sabinar (from [52]) – ISS 7a unit						
G. glycymeris	11	1.526±0.041	1.344±0.035	0.868±0.026	24.7±0.9	187+17/-14
S. bubonius	11	1.721±0.041	1.275±0.028	0.863±0.027	>>	188+18/-15
S. bubonius	10	0.118±0.003	1.200±0.035	0.829±0.026	>>	175+16/-14
Punta Sabinar (from [52]) – ISS 5e unit						
S. bubonius	4	1.177±0.029	1.154±0.031	0.715±0.026	>>	131+10/-9
S. bubonius	4	0.135±0.004	1.179±0.038	0.719±0.028	9.14±0.76	132+11/-10
(All values are quoted with 1 standard deviation)						

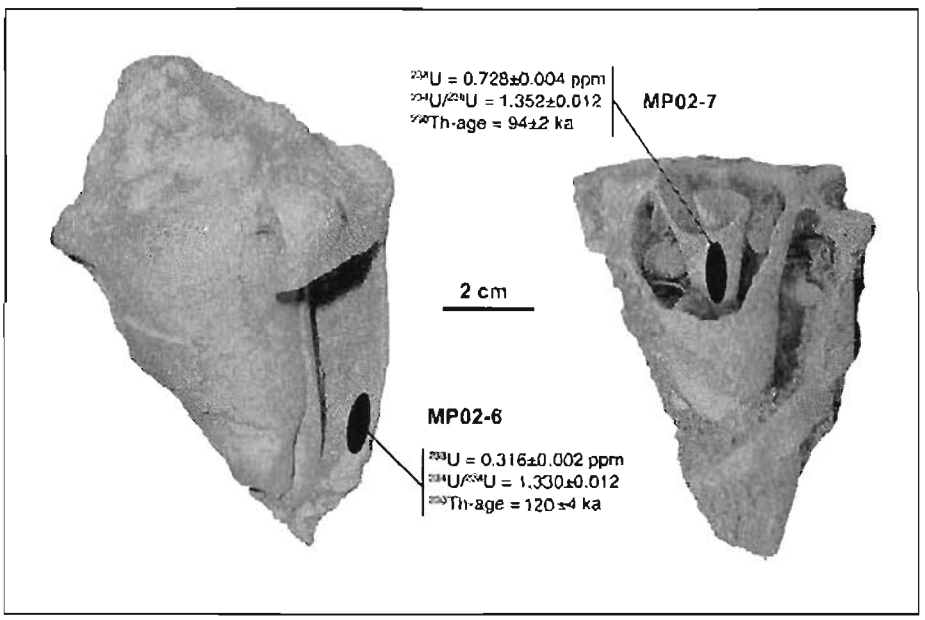

Figure 7.- U-series systematics in two *S. bubonius* specimens from the marine terrace T8 at La Marina-El Pinet assigned to OIS 5e. Note the enhanced late diagenetic U-incorporation in the most altered specimen (MP02-7) resulting in a much younger ^{230}Th-age.

^{230}Th-ages match increasing U concentrations. In comparison, at sites where early diagenetic cementation occurred, notably in beach rocks, mollusk shells including those of *S. bubonius*, usually depict more clustered ages and U-concentrations (*e.g.* [36], see also Table 3).

Nevertheless, in comparison with *S. bubonius* data from the OIS 5e sequence at La Marina-El Pinet, the set of ^{230}Th-ages yielded by the *C. caespitosa* specimens from the underlying unit (T7) illustrates a much closer geochemical system with relatively narrow clusters of ^{238}U-concentrations and activity ratios of daughter products (Table 1). When compared with modern specimens (Table 2), the fossil specimens show a somewhat lower ^{238}U concentration (with mean values of 2.736 ± 0.229 and 2.995 ± 0.266 μg/g respectively; both ±1σ). Two categories of processes may account for this difference:

i) A temperature control of the U/Ca ratio during aragonite precipitation. A higher temperature during the growth of the fossil specimens could account for their lower U content if one admits a temperature dependence of the U/Ca ratio in *C. caespitosa* similar to that observed by Min *et al.* [38] in the coral genus *Porites*, adding to the possibility of some influence of the ocean alkalinity over these ratios.

ii) Diagenetic effects that may include changes in U concentrations due to either U-mobility and/or secondary precipitation of some U-poor carbonate in the fossils. Such processes often result in less reliable U/Ca paleotemperatures in fossil corals than other tracers [39].

Proof for some post-depositional U-series fluxes in the fossil specimens of *C. caespitosa* is provided by their excess in ^{234}U, when compared with uranium from a purely marine origin (Fig. 9). This behaviour of U-series in fossil corals has been reported in most geological settings (e.g. [40, 41 and 42]. Here again, two mechanisms may account for this anomaly:

i) A diagenetic ^{234}Th (^{234}U)-^{230}Th-enrichment in the fossils, through still poorly understood processes frequently reported

Table 4: Model age limits of *Cladocora caespitosa* samples from La Marina

	Uncorrected age ± 2σ (ka)	Corrected (minimum) age with ^{234}U & ^{230}Th enrichment*	Corrected (maximum) age with diagenetic U-uptake**	Total U-content (ppm)	Maximum diagenetic U-percentage
MP01-1a	185.2+7.8/-7.2	164	220	2.598±0.011	17.9
MP01-1b	187.8+8.4/-7.7	156	251	2.755±0.013	29.9
MP01-1c	196.6+5.6/-5.3	168	255	2.458±0.011	25.6
MP01-1d	178.2+9.8/-8.9	170	200	2.915±0.023	12.5
MP01-2	239.8+18.4/-15.7	187	ns	2.737±0.021	—
MP02-1	207.6+11.4/-10.2	184	254	2.549±0.016	19.5
MP02-4	194.5+7.8/-7.2	168	243	3.234±0.017	22.8
MP02-5	189.5+8.8/-8.1	163	233	2.639±0.014	22
Mean values ± 1σ	191.3±8.7***	170±10	237±20		21.5±5

* Using the model developed by Thompson et al. [20]
** Constant diagenetic U-flux ($\delta^{234}Ui$ = 380‰) + authigenic U ($\delta^{234}Ui$ = 114.8‰; cf. Table 2 and appendix)
*** With the outlier MP01-2 excluded

in corals [40 and 20] as well as in mollusk shells [36]. As in the case of pre-Tyrrhenian fossils from the Mediterranean Sea illustrated by Hillaire-Marcel *et al.* [36], these processes lead eventually to situations beyond ^{230}Th-age limits where biogenic carbonates depict exceptionally high U contents with large excesses in ^{234}U and ^{230}Th (*i.e.*, activities well above secular equilibrium values with parent isotopes).

ii) A continuous or discontinuous late diagenetic U-uptake from ^{234}U-enriched pore-waters circulating in the deposits.

Any significant contamination of the samples by (^{232}Th-bearing) detrital particles can be discarded here in view of the measured $^{238}U/^{232}Th$ mass ratios (averaging 30, thus resulting in an activity ratio of about 100; Table 1). Assuming a $^{230}Th/^{232}Th$ activity ratio in the detrital fraction similar to that measured in marine clays (e.g., 0.5 in the North Atlantic [43]), this would result in a correction of a few hundred years on the samples' ages.

3.3. Open system age estimates

There is no reason to discard, for the study samples, the likeliness of a diagenetic $^{234}Th(^{234}U)$-^{230}Th-enrichment, a process that seems indeed ubiquitous in corals, but the second process (*i.e.*, the diagenetic addition of U) may have also played some role, in view of the high diagenetic U-uptake rates observed in fossil mollusks from the overlying deposits. For both processes, corrected ages can be estimated assuming constant rates through time. The first correction model is described in Thompson *et al.* [20], the second, in the Appendix. The first process results in apparent ^{230}Th-ages slightly younger than the true age of the fossils, whereas the second results in apparent ages older than their real age (Table 4).

The combination of both processes should result in corrected ^{230}Th ages intermediate between those yielded by the two (opposite) correction models, *i.e.*, ages probably not much different from those measured. One sample seems to provide some ground for such a conclusion: MP01-1d (Table 4) which shows minimum correction values in both ways (*i.e.*, 170 and 200 ka, respectively) with a measured apparent age of ~178 ka.

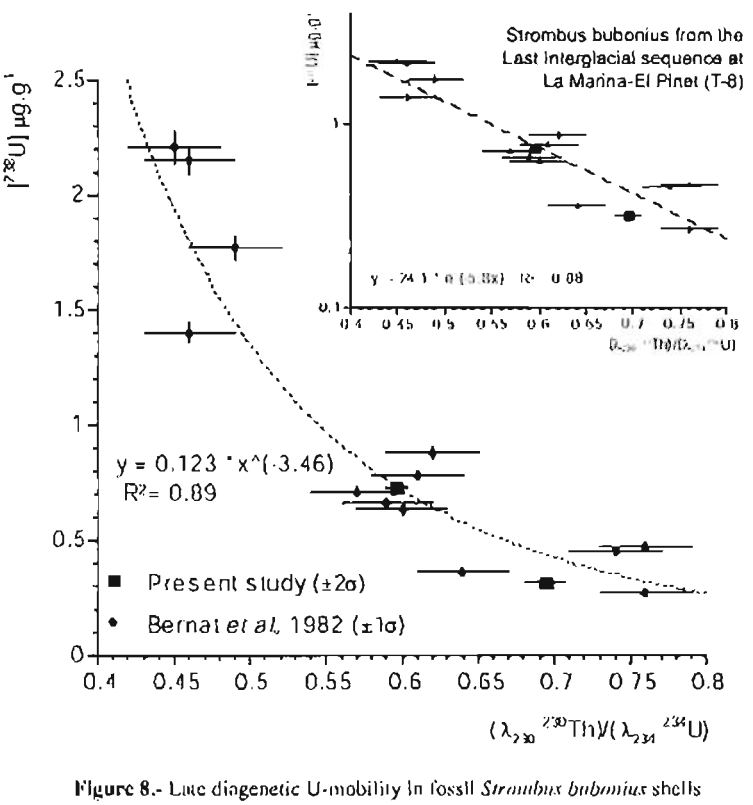

Figure 8.- Late diagenetic U-mobility in fossil *Strombus bubonius* shells originating from the Last Interglacial (LI) sequence at La Marina. Note

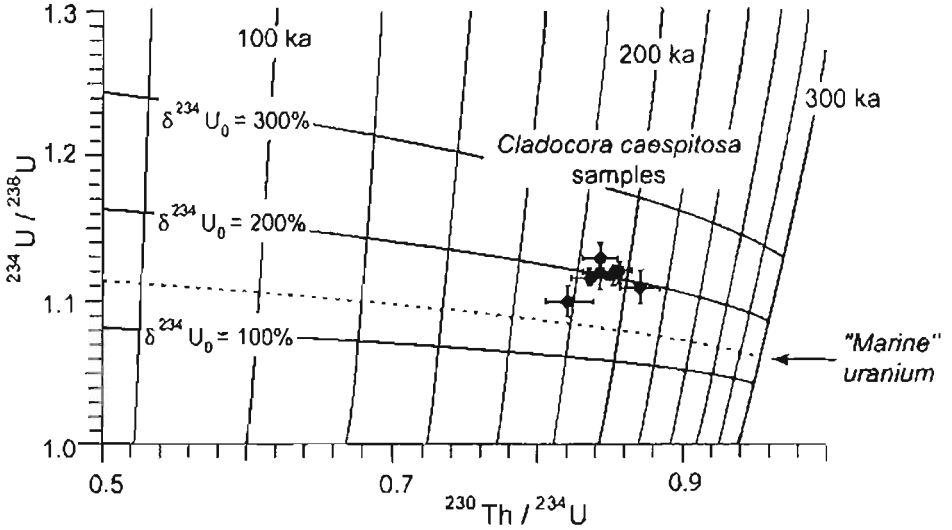

Figure 9.- Activity ratios coral samples from the marine terrace T7 at La Marina-El Pinet. Data indicate a light excess in ^{234}U *vs.* purely "marine" uranium, suggesting some diagenetic U-uptake and/or a more or less continuous ^{234}Th (^{234}U)-^{230}Th enrichment process. The outlier sample MP01-2 has not been plotted (see Table 1).

of last interglacial corals (3.51 ± 0.27 μg/g) indicates relatively high U/Ca ratios in *C. caespitosa* during warm episodes, such as OIS 5e, but also raises concerns about the reverse temperature dependence of these ratios in *C. caespitosa*, assumed above by analogy with the behaviour of *Porites* [38]. Indeed, the mean U content (3.51 ± 0.27 μg/g) of samples from the last interglacial, which is thought to be approximately 2° C warmer than the present interglacial [46], exceeds significantly ($\Delta = 0.52 \pm 0.38$ μg/g) that of the modern samples (2.995 ± 0.266 μg/g). Comparatively, the U content of OIS 7 samples seems low (2.736 ± 0.229 μg/g, n=8; see Table 1). Any significant diagenetic addition of U to these samples seems thus unlikely, and their true age should be closer to the minimum open system age of 170 ± 10 ka than to the maximum one of 237 ± 20 ka (Table 4).

Diagenetic U-uptake by the study samples was very likely lower than the maximum U-uptake value calculated in Table 4, because maximum U-uptake leads to calculate a very low initial U-content. In comparison with modern Mediterranean specimens (mean ^{238}U content of 2.995 ± 0.266 μg/g), the fossil corals show a lesser content (2.735 ± 0.245 μg/g). Higher temperatures during their growth could account for this difference [38], but if one subtracts also about 20% of U as in the maximum diagenetic U-uptake scenario, then the original content in authigenic U and the corresponding U/Ca ratio would be very low (appr. 2.15 μg/g and 0.9 μmoleU/moleCa). Such low values would very likely fall beyond reasonable estimates for the paleotemperature of OIS 7 interval in comparison with that of the Holocene (see also [40]). The drop from 1.26 μmoleU/moleCa in modern *C. caespitosa* to 0.9 μmole/mole for the corrected authigenic U/Ca ratio in the fossil specimens would indeed imply a growth temperature difference of appr. +9° C, assuming a U/Ca temperature dependence in *C. caespitosa* similar to that of *Porites*, for example. However, one cannot be totally conclusive here, because very low U contents have been observed in *C. caespitosa* skeletons of similar age from the eastern Mediterranean ([44] and Table 2).

For comparison purposes, Table 2 also shows α-counting measurements made by Szabo [in 45] on last interglacial samples of *C. caespitosa* from the western and central Mediterranean. These samples depict a mean U content of 3.51 ± 0.27 and an initial $\delta^{234}U$ value of 159 ± 6‰ (both ± 1σ). Their relatively low excess in ^{234}U with reference to the essentially "marine" signature of the uranium incorporated into the modern *C. caespitosa* skeletons ($\delta^{234}U = 148 \pm 4$; Table 2), suggests a reduced mobility of ^{238}U and/or its daughter isotopes in the corresponding samples (thus diagenetic conditions insuring a better closure of the radioactive system in comparison with those of the study site). Nevertheless, the mean ^{238}U content

Henceforth, besides an unequivocal assignment of these fossils (and of their embedding sediment) to OIS 7, one could tentatively discard an OIS 7e age, and retain an OIS 7a or 7c age for the corresponding maximum sea level. Sample MP01-1d, which shows the narrower difference between the two opposite corrections (*i.e.*, 170 and 200 ka; Table 4), would rather support an OIS 7a assignment.

4. The Tyrrhenian cycle and the "Senegalese" fauna chronostratigraphy

The term "Tirreno" (Tyrrhenian) was introduced by Issel [47] to describe the *Strombus bubonius*-bearing layers mentioned by Gignoux [48, 49] that encompassed the time span between the Sicilian and the Holocene. *S. bubonius* was usually accompanied with other warm species. This particular fossil assemblage was later named "Senegalese" fauna with reference to the present occurrence of its most characteristic taxa along the tropical shores of Senegal [50]. However the temporal extension of the Tyrrhenian as an chronostratigraphic unit, and the spreading pathway of its marker fauna still remain unclear. The Tyrrhenian is commonly assigned to the "Last Interglacial" *sensu lato* (OIS 5), and occasionally to the isotopic substage 5e [12, 51] notably in the central Mediterranean. However, large-scale geomorphological mapping assisted by U-series measurements on corals (this paper, Table 3) suggest that the "Senegalese" fauna including *S. bubonius* lived in the western Mediterranean during OIS 7 [32, 52] and, perhaps, as early as during interglacials OIS 9 or OIS 11 in the Spanish Mediterranean littorals [19]. The youngest occurrences of *S. bubonius* correspond to OIS 5c and, perhaps

OIS 5a [52, 53]. The sea surface temperature alkenone record from a deep sea core from the Alborán Sea off Almeria (Fig. 1B) shows that SST during OIS 7a was only 1° C lower than during OIS 5e [54].

In conclusion, the "Senegalese" can be seen as an endemic fauna in the western Mediterranean basin during preceding interglacials, but it did not survive the Würm glacial stage.

5. Chronostratigraphy of marine terraces in La Marina-El Pinet area

The marine terraces of La Marina (Fig. 2) can be associated to specific interglacial high sea levels using morphostratigraphical relationships and chronological data. Terrace T7 deposits with *Cladocora* and sparse *Strombus* accumulated during OIS 7, likely OIS 7a or 7c. The overlying terrace (T8) deposits are assigned to OIS 5e, according to stratigraphic, sedimentological and paleontological features, earlier U-series measurements [28, 32], and AAR data [29]. An additional criterion for this age assignment is that, in the "classical" quarry, terrace T8 includes at least two highstands, the older of which is oolitic, a distinctive lithology of the last interglacial marine sequences at regional scale [19].

Terrace T9 (Figs. 2 and 3) that gently cuts into the former sequences and also bears a warm water fauna is tentatively assigned to OIS 5c or 5a. The most recent terrace (T10) bears a fauna similar to the present-day one and is of Holocene age.

The well-cemented terrace T6 can not be dated positively but, according to its stratigraphic position, we suggest a possible OIS 9 age.

6. Paleo-sea levels and neotectonic implications

The altitudinal occurrence of the *C. caespitosa*-bearing marine unit raises the issue of the relative elevation of the OIS 7 and OIS 5 sea levels.

6.1. Maximum elevation of paleo-sea level during OIS 7 reported in literature

The elevation of OIS 5e paleo-sea level is relatively well constrained, because it is represented by the most ubiquitous and well-preserved set of littoral features along many coastlines of the world. Murray-Wallace and Belpeiro [2] deduced elevations of 2 m a.s.l. from exposures in southern Australia which are very similar to values found by Stirling *et al.* [3] in Western Australia, both considered to be located in tectonically stable coasts. A paleo-sea level of about 6m a.s.l. has been suggested by Chen *et al.* [4] and Kindler *et al.* [5] in the Bahamas. A similar elevation has been deduced by Muhs *et al.* [6] in Bermuda Island and Florida Keys.

Data on the relative elevation of sea level during OIS 7 are scarce and heterogeneous. Chappell and Shackleton [7] used marine oxygen isotope data to suggest a 15 m b.s.l. (below present sea level) position, whereas Roy and Boyd [8] placed it at 2-4 m a.s.l. in the stable South Australia. Later on, Murray-Wallace [9] concluded that, in this area, interglacial sea levels did not deviate more than 6 m from the present values during the past 11 interglacial. He also reported that faunas warmer than the modern ones were common in most pre-Holocene interglacial deposits.

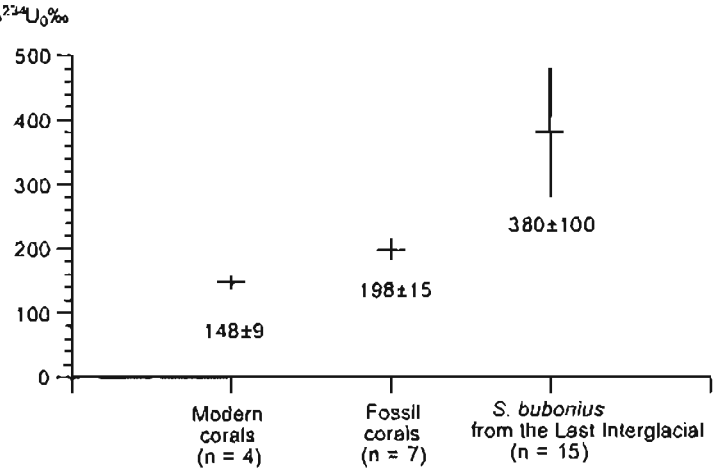

Figure 10.- Initial isotopic composition of uranium in modern vs. OIS 7 *Cladocora caespitosa* skeletons, compared with that of *Strombus bubonius* from OIS 5e deposits. The initial $\delta^{234}U$ value of *S. bubonius* shells (*i.e.*, 138‰) has been considered as representative of that of the "diagenetic uranium" incorporated into fossil coral skeletons and that of the modern Mediterranean *C. caespitosa* samples (*i.e.*, 148‰) for their authigenic "marine" fraction of their uranium.

Ramsay and Cooper [10] reported elevations of 3 m b.s.l. for OIS 7a deposits in South Africa concluding that sea level during the penultimate interglacial was likely close to the present one. Shorelines of OIS 5e and OIS 5c episodes appear to be around 4 m a.s.l. in the same area.

Kindler *et al.* [5] identified a paleo-sea level close to modern datum during OIS 7 in the Bahamas. In opposition, Schellmann and Radtke [11] reported values of 16 m b.s.l. for OIS 7a and 3 m b.s.l. for OIS 7c around Barbados (based on the 2 m a.s.l. sea level of OIS 5e).

At Tomasso Natale (Sicily, Italy), Hearty *et al.* [12] found *Cantharus viverratus*, a "Senegalese" form, among corals dated at 250 ka and *Arca* shells that yield aminogroup F ratios. The authors also deduced that "aminogroup F deposits are present at elevations similar to that of aminogroup E deposits. *Strombus* may be associated with both aminogroups, but unequivocal data have emerged only from last-interglacial deposits".

Recently, Bard *et al.* [13] set an OIS 7a (202-190 ka) minimum sea level at 18.5 m b.s.l. based on high precision U-series measurements in a submerged stalagmite from the Argentarola Cave (Italy). They conclude with reference to other studies [14, 15, 16], that the maximum sea level of this interval had not exceeded -9 m below the present one. If this is true, then one should perhaps consider a 7c age for the deposits of terrace T7. However, we prefer to keep open

the possibility that for a short time interval of OIS 7a, a much higher sea stand may have been attained. Comments from Winnograd [17] based on data from Harmon *et al.* [18], about the possibility of an underestimation of the paleo-sea level elevation during OIS 7a by Li *et al.* [15] would go along our own conclusion.

More in accordance with the present study, Poole *et al.* [44] report *C. caespitosa*-bearing marine units from southern Cyprus at elevations 8-11 m a.s.l. (185-192 ka) and <3m a.s.l. (116-130 ka).

Closer to our study area, Zazo [55] and Zazo *et al.* [19] suggested that sea level during OIS 7 in the western Mediterranean was generally lower (but not much different) than that of OIS 5e. Vessica *et al.* [56] used stable isotopes and U-series analyses of calcite overgrowths and speleothems found between 40 m a.s.l. and 0 m in Mallorca (Balearic Islands, Fig. 1) to recognize sea high stands matching respectively OIS 9 or older, OIS 7 (231 ± 28 ka, at 4.2 m a.s.l.), OIS 5e (2.5 m a.s.l.), OIS 5c, and OIS 5a.

6.2. *New constraints on the maximum elevation of OIS 7 sea level from La Marina-El Pinet data*

The literature survey does not offer unequivocal conclusions about a precise maximum elevation of sea-level during OIS 7. Unfortunately, the coastal area of La Marina-El Pinet shows some tectonic instability. The topographic elevations of the inner margin of all marine terraces on both sides of the fault line (Figs. 2 and 3) provide evidence for this. Terrace T8, assigned to OIS 5e, occurs at 8 m a.s.l. in the upthrown block, whereas its elevation in the downthrown block does not exceed 5.5 m a.s.l. (Figs. 2 and 3). The elevation of the inner margin of terrace T7, that bears *C. caespitosa* and *S. bubonius*, is more difficult to assess. Facies analysis and faunal content (*Cladocora* and its accompanying fauna) in Terrace T7 allow an estimation of water depth. *Cladocora caespitosa* (L.) is the main native zooxantellate and constructional coral of the Mediterranean Sea and its hemispherical colonies (Fig. 4B 1 and 2) form patches in the shoreface (4 to 10 m), but become rare between 10 m and 40 m of water depth [57]. This range is far too large to infer precise paleo-sea level elevations, but the co-occurrence of well preserved littoral faunas in the same beds suggests a limited reworking and somewhat restricts the range in this particular case to the upper shoreface. Setting the shallowest margin (4 m) as the real water depth in which fossil *Cladocora* lived, we speculate that the elevation of the inner margin of T7 would not deviate by more than 2-3 m from that of T8, implying that sea levels during OIS 7a or 7c and OIS 5e did not differ much from each other. An additional argument for the assumed water depth is that at present *S. latus* Gmelin (*S. bubonius* Lamark) lives at 4 m water depth in protected shores of Ilha do Sal (Cape Verde Islands) [58].

Assuming the mean sea level of approximately 2 m a.s.l. during OIS 5e calculated in areas tectonically stable and far from the former ice sheets [3], and constant vertical tectonic movements, we deduce uplift rates of 0.025 mm/yr and 0.044 mm/yr for the downthrown and upthrown blocks, respectively, during the last ~ 125 ka. Extending these rates to the last 195 ka, a maximum sea level position approximately one metre below the present could then be estimated for OIS 7a (possibly for OIS 7c depending on the final assignment of the *C. caespitosa* bearing unit). Such a value for the maximum sea level of OIS 7 is in agreement with the data from other coastal areas of Spain cited above [19].

7. Conclusions

The sequence of Quaternary marine terraces at La Marina-El Pinet is one of the best-studied for recognizing both the chronology of its faunal content and the elevation of paleo-sea levels during the penultimate and last interglacials in the western Mediterranean basin. It illustrates the altitudinal relationship between the maximum sea level stands of OIS 7 (likely 7a, possibly 7c) and OIS 5e, suggesting that the maximum sea level of OIS 7 should not have been much lower than the modern sea level.

From a paleoecological view point, both the Mediterranean scleractinian coral *C. caespitosa* and the "Senegalese" fauna were present during the last and penultimate interglacials in the area. In terrace T7 (OIS 7), *C. caespitosa* forms relatively large colonies whereas the "Senegalese" fauna, including *S. bubonius*, is scarce. In contrast, the overlying terrace T8, with its basal oolitic sub-unit characteristic of OIS 5e along the Spanish coasts, bears an abundant "Senegalese" fauna, including *S. bubonius*, but scarce remains of *C. caespitosa*. These features seems thus to be representative at regional scale probably due –among other causes- to higher SST (~1° C) during OIS 5e in comparison with OIS 7 [54].

Finally, we consider that a maximum sea level of short duration culminating near present sea level, during either 7a or 7c, would not be incompatible with the occurrence of better developed but significantly lower elevation deposits emplaced during longer duration high sea stands of OIS 7. It seems thus likely that most values reported for OIS 7 paleo-sea levels in literature, are not as conflicting as they may appear from a quick survey of the literature (see for example [17 and 56]), but simply represent various standstills of this interglacial. Because of their relatively short duration suggested by the SPECMAP curve, the maximum sea levels intervals may have left poorer records, more easily reworked, than some lower elevation marine features of the same interglacial. Improvements in age estimates may help to set ultimately a paleo-sea level curve spanning the penultimate interglacial. From this view point, as put forth by Thompson [20], the open system age model that has been used in the present paper, as well as better assessments of diagenetic U-fluxes, may be a help

Acknowledgements

Research financed by Spanish Projects BTE2002-1691 and 1065, CGL-2005-04655/BTE, and CGL-2005-01336/BTE. Thanks are due to Pascal Kindler and Luc Ortlieb for their comments and suggestions. This paper is a contribution to IGCP Project 495 (*Quaternary Land-Ocean Interactions: Driving mechanisms and Coastal Responses*) and INQUA Coastal and Marine Processes. CHM acknowledges financial support from the Science and Engineering Research Council of Canada and the UNESCO Chair for Global Change Study of *Université du Québec à Montréal*.

Appendix: Model ^{230}Th age calculations

i) Continuous addition of ^{234}Th (^{234}U) and ^{230}Th (see [20])

This model yields here, when using the mean activity ratios measured in the *C. caespitosa* samples, a corrected (and minimum) age of 168 ± 9.5 ka (see Table 4).

ii) Continuous diagenetic addition of U from pore water with a constant U flux

It is represented by the following set of linear differential equations:

(1) $$\frac{d^{238}U}{dt} = \Phi_{238}(t) - \left(\lambda_{238} * {}^{238}U\right) \approx \Phi_{238}(t) \quad \text{since } \lambda_{238} << \Phi_{238}$$

Where

λ_{238} = ^{238}U decay constant

Φ_{238} = diagenetic ^{238}U flux (*e.g.*, in dpm/g.ka if ^{238}U is in dpm/g and λ in ka^{-1})

(2) $$\frac{d^{234}U}{dt} = -\lambda_{234}\,{}^{234}U + \lambda_{238}\,{}^{238}U + \Phi_{234}(t)$$

where λ_{234} = ^{234}U decay constant

Φ_{234} = diagenetic ^{234}U flux (*e.g.*, in dpm/g.ka if ^{234}Ud in dpm/g and λ in ka^{-1}) such as $\Phi_{234}/\Phi_{238} = {}^{234}Ud/{}^{238}Ud$ = activity ratio of diagenetic "d" pore water U; here $^{234}Ud/^{238}Ud = 1.39$.

(3) $$\frac{d^{230}Th}{dt} = -\lambda_{230}\,{}^{230}Th + \lambda_{234}\,{}^{234}U$$

where λ_{230} = decay constant of ^{230}Th.

Integrating (1) yields:

(4) $$^{238}U(t) = {}^{238}U(0) + \int_0^t \Phi_{238}(t')dt'$$

We may now rewrite (2) as:

(5) $$\frac{d^{234}U}{dt} = \lambda_{234}\,{}^{234}U + f(t)$$

where

(6) $$f(t) = -\lambda_{238}\,{}^{238}U + \Phi_{234}(t)$$

The general solution to (5) is:

(7) $$^{234}U(t) = \left[{}^{234}U(0) * \exp(-\lambda_{234} * t)\right] + \left[\exp(-\lambda_{234} * t) * \int_0^t \exp(\lambda_{234} * t') * f(t_*) * dt'\right]$$

Integrating by parts the second term on the right hand side of (7) yields:

$$(8)\quad {}^{234}U(t) = \left[{}^{234}U(0) * \exp(-\lambda_{234} * t)\right] + \left[\frac{1}{\lambda_{234}} * \left[f(t) - (\exp(-\lambda_{234} * t) * f(0))\right]\right] - \left[\frac{\exp(-\lambda_{234} * t)}{\lambda_{234}} \int_0^t \exp(\lambda_{234} * t) * \left(\frac{df}{dt'}\right) * dt'\right]$$

Equation (3) is similar in form to (5) and in analogy to the solution (7), we obtain:

$$(9)\quad {}^{230}Th(t) = \left[{}^{230}Th(0) * \exp(-\lambda_{230} * t)\right] + \left[\exp(-\lambda_{230} * t) * \int_0^t \exp(\lambda_{230} * t') * \left(\lambda_{234} * {}^{234}U(t')\right) * dt'\right]$$

Assuming that the flux $\Phi_{238}(t)$ is constant in time, then (4) simplifies into:

$$(10)\quad {}^{238}U(t) = {}^{238}U(0) + (\Phi_{238} * t)$$

In a similar fashion, assuming that $\Phi_{234}(t)$ is constant in time and using expressions (6) and (10), we may then rewrite expression (8) as:

$$(11)\quad {}^{234}U(t) = \left[{}^{234}U(0) * \exp(-\lambda_{234} * t)\right] + \left[\frac{\lambda_{238}}{\lambda_{234}} * \Phi_{238}\right] + \left[\frac{\lambda_{238}}{\lambda_{234}} * \left({}^{238}U(0) + \frac{\Phi_{234}}{\lambda_{238}} - \frac{\Phi_{238}}{\lambda_{234}}\right) * \left(1 - \exp(-\lambda_{234} * t)\right)\right]$$

Substituting (11) into (9), we finally obtain the expression (12) below:

$$(12)\quad {}^{230}Th(t) = \left[{}^{230}Th(0) * \exp(-\lambda_{230} * t)\right] + \left[\frac{\lambda_{238}}{\lambda_{230}} * \Phi_{8} * t\right] + \left[\frac{\lambda_{238}}{\lambda_{230}} * \left[{}^{238}U(0) + \frac{\Phi_{234}}{\lambda_{238}} - \left(\Phi_{238} * \left(\frac{1}{\lambda_{234}} + \frac{1}{\lambda_{230}}\right)\right)\right] * \left[1 - \exp(-\lambda_{230} * t)\right]\right] + \left[\left[\frac{\lambda_{234}}{\lambda_{230} - \lambda_{234}}\right] * \left[{}^{234}U(0) - \left(\frac{\lambda_{238}}{\lambda_{234}} * \left({}^{234}U(0) + \left(\frac{\Phi_{234}}{\lambda_{238}} - \frac{\Phi_{238}}{\lambda_{234}}\right)\right)\right)\right] * \left[\exp(-\lambda_{234} * t) - \exp(-\lambda_{230} * t)\right]\right]$$

A simplified quasi-arithmetic approach can also be followed.

$$(13)\quad \delta a = \delta a_0 \exp(-\lambda_{234} * t)$$

$$(14)\quad \delta d = \delta d_0 \exp(-\lambda_{234} * t)$$

where:

$\delta = \delta^{234}U = [({}^{234}U/{}^{238}U) - 1] * 10^3$

δ_0: the isotopic composition at the origin (here $\delta^{234}Ua = 148‰$ and $\delta^{234}Ud = 380‰$; see Fig. 10)

a, the authigenic fraction

d, the diagenetic fraction

then, from equations (13) and (14):

(15) $f_a = (\delta m - \delta d)/(\delta a - \delta d)$ when $f_d = 1 - f_a$

with f_a and f_d standing respectively for the authigenic and diagenetic fractions of ^{238}U, and δm, for the measured isotopic composition of uranium.

Furthermore:

$$(16)\ \frac{\lambda_{230}{}^{230}\mathrm{Thd}}{\lambda_{238}{}^{238}\mathrm{Ud}} = (1 - e^{-\lambda_{230}t}) + \left(\frac{\lambda_{234}{}^{234}\mathrm{Ud}}{\lambda_{238}{}^{238}\mathrm{Ud}} - 1\right)\left(\frac{\lambda_{230}}{\lambda_{230} - \lambda_{234}}\right)\left(1 - e^{-(\lambda_{230} - \lambda_{234})t}\right)$$

$$(17)\ \frac{\lambda_{230}{}^{230}\mathrm{Tha}}{\lambda_{238}{}^{238}\mathrm{Ua}} = (1 - e^{-\lambda_{230}t}) + \left(\frac{\lambda_{234}{}^{234}\mathrm{Ua}}{\lambda_{238}{}^{238}\mathrm{Ua}} - 1\right)\left(\frac{\lambda_{230}}{\lambda_{230} - \lambda_{234}}\right)\left(1 - e^{-(\lambda_{230} - \lambda_{234})t}\right)$$

Then, incremental values of "t" are introduced into equations 13, 14, 16 and 17, until:

$$(18)\ \left[\frac{\lambda_{230}{}^{230}\mathrm{Thm}}{\lambda_{238}{}^{238}\mathrm{Um}}\right] - \left[\left(\mathrm{fd} * \frac{\lambda_{230}{}^{230}\mathrm{Thd}}{\lambda_{238}{}^{238}\mathrm{Ud}}\right) + \left(\mathrm{fa} * \frac{\lambda_{230}{}^{230}\mathrm{Tha}}{\lambda_{238}{}^{238}\mathrm{Ua}}\right)\right] = 0$$

with $(\lambda_{230}{}^{230}\mathrm{Thm}/\lambda_{238}{}^{238}\mathrm{Um})$ standing for the measured $^{230}Th/^{238}U$ activity ratio.

In the present case, with the activity ratios measured in the *C. caespitosa* samples, a mean "t" value of 237 ± 20 (±1σ) can be set for the (maximum) corrected age.

References

[1] Bard E., Hamelin B., Fairbanks R.G., Zindler A., Arnold M., Mathieu G., U/Th and ^{14}C ages of corals from Barbados and their use for calibrating the ^{14}C timescale beyond 9000 years BP, Nuclear Instrum. Methods B 52 (1990) 461-468.

[2] Murray-Wallace C., Belperio A.P., The last interglacial shoreline in Australia –a review, Quaternary Sci. Rev. 10 (1991) 441-461.

[3] Stirling, C.H., Esat, T.M., Lambeck, K., McCulloch, M.T., Timing and duration of the last interglacial: evidence for a restricted interval of widespread coral reef growth, Earth Planet. Sci. Lett. 160 (1998) 745-762.

[4] Chen, J.H., Curran, H.A., White, B., Wasseburg, G.J., Precise chronology of the last interglacial period: ^{234}U-^{230}Th data from fossil coral reefs in the Bahamas, Geol. Soc. Am. Bull. 103 (1991) 82-97

[5] Kindler, P., Reyss, J.L., Cazala, C., Plagnes, V., Discovery of a composite reefal terrace of middle and late Pleistocene age in Great Inagua Island, Bahamas. Implications for regional tectonics and sea-level history, Sedimentary Geology (2006), in press.

[6] Muhs D.R., Simmons K.R., Steinke B., Timing and warmth of the Last Interglacial period: new U-series evidence for Hawaii and Bermuda and a new fossil compilation for North America, Quaternary Sci. Rev. 21 (2002) 1355-1383.

[7] Chappell J., Shackleton N.J., Oxygen isotopes and sea level, Nature 324 (1986) 137-140.

[8] Roy P.S., Boyd R., Quaternary Geology of a tectonically stable, wave dominated, sediment-deficient margin, Southeast Australia. IGCP Project 367, Field Guide to the Central South Wales Coast. New south Wales Geological Survey, Sydney, 1996, 174 p.

[9] Murray-Wallace, C. Pleistocene coastal stratigraphy, sea-level highstands and neotectonism of the southern Australian passive continental margin – a review, Journal of Quaternary Science 17 (2002) 137-140.

[10] Ramsay P.J., Cooper J.A.G., Late Quaternary sea-level change in South Africa, Quaternary Res. 57 (2002) 82-90.

[11] Schellmann G., Radtke A., A revised morpho-and chronostratigraphy of the Late and Middle Pleistocene coral reef terraces on Southern Barbados (West Indies), Earth-Sci. Rev. 64 (2004) 157-187.

[12] Hearty P.J., Miller G.H., Stearns C.E., Szabo B.J., Aminostratigraphy of Quaternary shorelines in the Mediterranean basin, Geol. Soc. Am. Bull. 97 (1986) 850-858.

[13] Bard E., Antonioli F., Silenzi S., Sea-level during the penultimate interglacial period based on a submerged stalagmite from Argentarola Cave (Italy), Earth Planet. Sci. Lett. 196 (2002) 135-146.

[14] Lundberg J., U-series dating of carbonates by mass spectrometry with examples of speleothem, coral and shell, Ph.D. thesis, McMaster University, Hamilton, ON, 1990, 271 p.

[15] Li W.X., Lundberg J., Dickin A.P., Ford D.C., Schwarcz H.P., McNutt R., Williams D., High-precision mass-spectrometric ura-

nium-series dating of cave deposits and implications for paleoclimate studies, Nature 339 (1989) 534-536.
[16] Lundberg J., Ford D.C., Schwarcz H.P., Dickin A.P., Li W.X., Dating sea level in caves. Response to comment by I.J. Winograd, Nature 343 (1990) 217-218.
[17] Winnograd I.J., Dating sea level in caves, Nature 343 (1990) 217.
[18] Harmon R.S., Mitterer R.M., Kriausakul N., Land L.S., Schwarcz H.P., Garrett P., Larson G.J., Leonard Vacher H., Rowe M., U-series and amino-acid racemization geochronology of Bermuda: Implications for eustatic sea-level fluctuation over the past 250,000 years Palaeogeogr. Palaeoclim. Palaeoecol. 44 (1983) 41-70.
[19] Zazo C., Goy J.L., Dabrio C.J., Bardají T., Hillaire-Marcel C., Ghaleb B., González-Delgado A., Soler V., Pleistocene raised marine terraces of the Spanish Mediterranean and Atlantic coasts: records of coastal uplift, sea-level highstands and climate changes, Mar. Geol. 194 (2003) 103-133.
[20] Thompson W.G., Spiegelman M.W., Goldstein S.L., Speed R.C., An open-system model for U-series age determinations of fossils corals, Earth Planet. Sci. Lett., 210 (2003) 365-381.
[21] Imbrie J., Hays J.D., Martinson D.G., McIntyre A., Mix A.C., Morley J.J., Pisias N.G., Prell W.L., Shackleton N.J., The orbital theory of Pleistocene climate: support from a revised chronology of the marine $\delta^{18}O$ record, in: Berger A.L. *et al.* (Eds.), Milankovitch and Climate, Part 1, Reidel, 1984, pp. 269-305.
[22] Martinson D.G., Pisias N.G., Hays J.D., Imbrie J., Moore T.C., Shackleton N.J., Age dating and the orbital theory of the ice ages: development of a high-resolution 0 to 300,000-year chronostratigraphy, Quat. Res. 27 (1987) 1-29.
[23] Chappell J., Omura A., Esat T., McCulloch M., Pandolfi J., Ota Y., Pillans B., Reconciliation of late Quaternary sea levels derived from coral terraces at Huon Peninsula with deep sea oxygen isotope records, Earth Planet. Sc. Lett. 141 (1996) 227-236.
[24] Fruijtier C., Elliott T., Schluger W., Mass-spectrometric U-234-Th-230 ages from the Key Largo Formation, Florida Keys, United States: Constraints on diagenetic age disturbance, Geol. Soc. Amer. Bull. 112 (2000) 267-277.
[25] Goy J.L., Zazo C., Sequences of the Quaternary marine levels in Elche Basin (Eastern Betic Cordillera, Spain), Palaeogeography, Palaeoclimatology, Palaeoecology 68 (1988) 301-310.
[26] Goy J.L., Zazo C., The role of neotectonics in the morphologic distribution of the Quaternary marine and continental deposits of the Elche Basin, southeast Spain. Tectonophysics 163 (1989) 219-225.
[27] Cuerda J., Los tiempos cuaternarios en Baleares, Conselleria de Cultura, Educació i Esports, Govern Balear, 1989, 310 p.
[28] Bernal M., Echaüller J.V., Busquet J.C., Novelles datations I_o-U sur des Strombes du Dernier Interglaciaire en Méditerranée, Comptes Rendus des Séances de l'Academie des Sciences Paris II 295 (1982) 1023-1026.
[29] Hearty P.J., Hollin J.T., Dumas B., Geochronology of Pleistocene littoral deposits on the Alicante and Almería coasts of Spain, Trabajos sobre Neógeno-Cuaternario 10 (1987) 95-107.
[30] Goy J.L., Zazo C., Bardají T., Somoza L., Causse C., Hillaire-Marcel C., Eléments d'une chronostratigraphie du Tyrrhénien des régions d'Alicante-Murcia, Sud-est de l'Espagne, Geodin. Acta 6-2 (1993) 103-119.
[31] Montenat, C., Les formations néogènes et quaternaires du Levant espagnol. Thèse d'Etat. Univ. Paris Orsay, 1973, 1170 p.
[32] Causse Ch., Goy J.L., Zazo C., Hillaire-Marcel C., Potentiel chronologique (Th/U) des faunes Pléistocènes méditerranéennes: exemple des terrasses marines des régions de Murcie et Alicante (Sud-est de l'Espagne), Geodin. Acta 6-2 (1993) 121-134.
[33] Cook H.E., Johnson P.D., Matti J.C., Zemmels I., Methods of sample preparation and X-ray diffraction data analysis, X-ray Mineralogy Laboratory, Deep Sea Drilling Project, University of California, Riverside, in: Hayes D.E., Frakes L.A., *et al.* (Eds.), Init. Repts. DSDP, 28, U.S. Govt. Printing Office, Washington, 1975, pp. 999-1007.
[34] Goldsmith J.R., Graf D.L., Relations between lattice constraints and composition of the Ca-Mg carbonates, Am. Mineral. 43 (1958) 84–101.
[35] Edwards R.L., Chen J.H., Wasserburg G.J., ^{238}U-^{234}U-^{230}Th-^{232}Th systematics and the precise measurement of time over the past 500,000 years, Earth Planet. Sci. Lett. 81 (1987) 175-192.
[36] Hillaire-Marcel C., Gariepy C., Ghaleb B., Goy J.L., Zazo C., Cuerda J., U-series measurements in Tyrrhenian deposits from Mallorca. Further evidence for two last Interglacials high sea-levels in the Balearic Islands, Quaternary Sci. Rev. 15 (1996) 53-62.
[37] Pons-Branchu E., Hillaire-Marcel C., Deschamps P., Ghaleb B., Sinclair D., Dating and early diagenetic evolution of a recent deep sea coral (*Lophelia pertusa*) from the Eastern Atlantic (Sea of the Hebrides) inferred from U-Th-^{226}Ra and ^{14}C systematics. Geochim. Cosmochim. Acta 69 (2005) 4865-4879.
[38] Min G.R., Edwards R.L., Taylor F., Recy J., Gallup C.D., Beck J.W., Annual cycles of U/Ca in coral skeletons and U/Ca thermometry, Geochim. Cosmochim. Ac. 59 (1995) 2025-2042.
[39] Castelluro C., Hamelin B., Montaggioni L., Juillet-Leclerc A., Récy J., Sr/Ca and U/Ca in a Pleistocene *Porites* from New Caledonia: Was the Last Interglacial cooler than Present?, Abstracts, Symposium B-06: *New approaches in estimating marine and continental paleotemperatures for the Cainozoic*. European Union of Geosciences meeting, Nice, France, 1999.
[40] Gallup C., Edwards R.L., Johnson R.G., The timing of high sea levels over the past 200,000 years, Science 263 (1994) 796-800.
[41] Hamelin B., Bard E., Zindler A., Fairbanks R.G., $^{234}U/^{238}U$ mass spectrometry of corals: How accurate is the U-Th age of the last interglacial period?, Earth Planet. Sci. Lett.106 (1991) 169-180.
[42] Bard E., Fairbanks R.G., Hamelin B., Zindler A., Hoang C.T., Uranium-234 anomalies in corals older than150,000 yr, Geochim. Cosmochim. Ac. 55 (1991) 2385-2390.
[43] Veiga-Pires C., Hillaire-Marcel C., U and Th isotope constraints on the duration of Heinrich events H0-H4 in the southeastern Labrador Sea, Paleoceanography 14 (1999) 187-199.
[44] Poole A.J., Shimmield G.B., Robertson A.H.F., Late Quaternary uplift of the Troodos ophiolite, Cyprus: Uranium-series dating of Pleistocene coral, Geology 18 (1990) 894-897.
[45] Hearty P.J., An Inventory of Last Interglacial (sensu lato) Age Deposits from the Mediterranean Basin, Z. Geomorphol. 62 (1986) 51-69.
[46] White J.W.C., Don't touch that dial, Nature 364 (1993) 186.
[47] Issel A., Lembi fossiliferi quaternari e recenti nella Sardegna meridionale, Accademia Nazionale dei Lincei, Serie 5-23 (1914) 759-770.
[48] Gignoux M., Les couches à Strombus bubonius (Lmk) dans la Méditerrnée occidentale, C. R. Séances Acad. Sciences, February 6th (1911) 1-3.
[49] Gignoux M., Les formations marines pliocenes et quaternaires de l'Italie du sud et de la Sicile, Ann. Univ. Lyon 36, (1913).
[50] Bonifay E., Mars P., Le Tyrrhénien dans le cadre de la chronologie quaternaire méditerranéenne, Bull. Soc. Géol. Fran. Série 7-1 (1963) 62-78.
[51] McLaren S.J., Rowe P.J., The reability of Uranium-series mollusc dates from the western Mediterranean basin, Quaternary Sci. Rev. 15 (1996) 709-717.
[52] Hillaire-Marcel C., Carro O., Causse C., Goy J.L., Zazo C., Th/U dating of *Strombus bubonius* bearing marine terraces in southeastern Spain, Geology 14 (1986) 613-616.
[53] Bernal M., Bousquet J.C., Dars R., Io-U dating of the Ouljian stage from Torre García (Southern Spain), Nature 275 (1978) 301-303.
[54] Martrat, B., Grimalt, J.O., López-Martínez, C., Cacho, I., Sierro, F.J., Flores, J.A., Zahn, R., Canals, M., Curtis, J.H., Hodell, D.A., Abrupt Temperature Changes in the Western Mediterranean over the Past 250,000 Years. Science 306 (2004) 1762-1765.
[55] Zazo C., Interglacial Sea levels, Quat. Int. 55 (1999) 101-113
[56] Vessica P.L., Tuccimei P., Turi B., Fornós J.J., Ginés A., Ginés J., Late Pleistocene paleoclimates and sea-level change in the Mediterranean as inferred from stable isotope and U-series studies

of overgrowths on speleothems. Mallorca, Spain. Quaternary Sci. Rev.19 (2000) 865-879.
[57] Peirano A., Morri C., Bianchi C.N., Aguirre J., Antonioli F., Calzetta G., Carobene L., Mastronuzzi G., Orrù P., The Mediterranean coral *Cladocora caespitosa*: a proxy for past climate fluctuations? Global Planet. Change 40 (2004) 195-200.
[58] Morri, C.R., Cattaneo-Vietti, G., Sartoni, G., Bianchi, N., Shallow epibentic communities of Ilha do Sal (Cape Verde Archipelago, Eastern Atlantic). Arquipélago. Life and Marine Sciences, Ponta Delgada, Açores. Supplement 2 (Part A) (2000) 157-165.